J. Geomag. Geoelectr., 49, 801–806, 1997

Data-Adaptive Inversion of the Oklahoma EMAP Dataset

Yasuo OGAWA[1,2]

[1] Geological Survey of Canada, 1 Observatory Crescent, Ottawa, Ontario K1A 0Y3, Canada
[2] Geological Survey of Japan, 1-1-3 Higashi, Tsukuba, Ibaraki 305, Japan

(Received March 6, 1995; Revised August 23, 1996; Accepted January 11, 1997)

The Oklahoma EMAP dataset was analyzed using a two-dimensional inversion algorithm which includes static shifts as free parameters. Model misfit was minimized while simultaneously minimizing the resistivity roughness norm and the static shift $L2$ norm. The tradeoff parameters between the model misfit and these two norms were determined to minimize the Akaike's Bayesian Information Criterion (ABIC).

1. Introduction

The objective of the Oklahoma EMAP survey was to map the subsurface distribution of a sedimentary layer through surface inhomogeneity. The objective of this paper is to apply recent techniques in inversion of MT data to that dataset in order to elaborate the interpretation.

The nature of the dataset is reviewed by Jones and Schultz (1997). Briefly, the dataset consists of 93 electric dipoles aligned in one direction for an EMAP survey. Accordingly, only TM mode data are available from impedance component Z_{xy}, where x is the direction parallel to the profile. Dipole separation ranges from 149 m to 1089 m and the typical dipole lengths range between 220 and 250 m. The observation frequency (period) range is from 384 Hz to 0.00055 Hz (1820 s).

2. Two-Dimensional Inversion Scheme

A two-dimensional inversion was applied to the TM mode data (Z_{xy}), based on the work of Ogawa and Uchida (1996) and Ogawa (1997). An outline of the idea is described below.

The model uses finite element elements, of rectangular shape, grouped into regularization blocks. The static shifts were taken as model parameters, similar to the approach of deGroot-Hedlin (1991). Accordingly, the model parameters m are written as follows.

$$m = \begin{bmatrix} m_{\rho,\ block} \\ g_{site} \end{bmatrix}, \tag{1}$$

where m_ρ denotes the $\log_{10}$(resistivity) of the regularization blocks. The static shift at each site, g_{site}, is defined using observed (distorted) apparent resistivity ρ_a^{obs} and undistorted apparent resistivity ρ_a^{undist} (free from static shift) as.

$$g_{site} = \log_{10} \rho_a^{obs} - \log_{10} \rho_a^{undist}. \tag{2}$$

The model misfit is defined as

$$S(m) = |Wd - WF(m)|^2 \tag{3}$$

where, d, W, and F denotes the data, reciprocal of the standard error of the data, and theoretical response for that site, as a function of m. S can be approximated by S_0 using the model parameters of the previous iteration m_{old} and Jacobian matrix A.

$$S(m) \approx S_0(m) = \left|W\tilde{d} - WAm\right|^2 \tag{4}$$

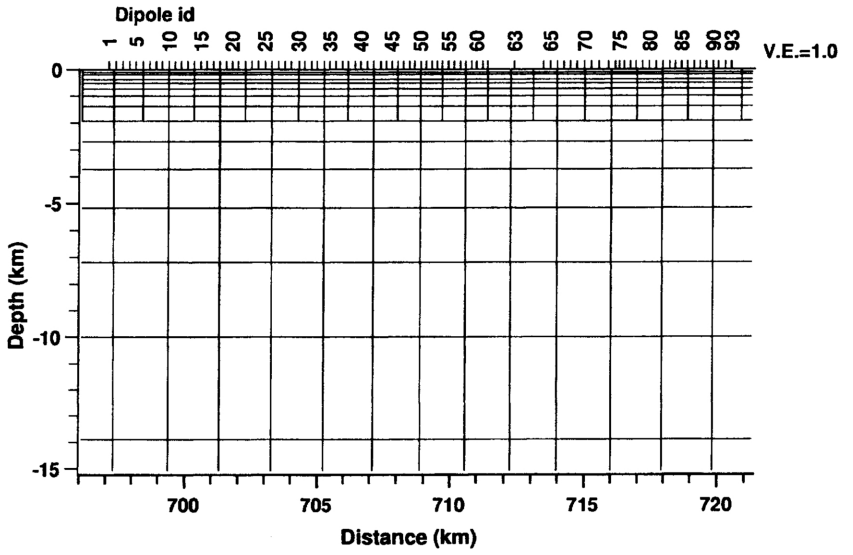

Fig. 1. Regularization blocks for the model. On the surface the dipole locations are shown by ticks. The dipoles are represented by point dipoles in this study.

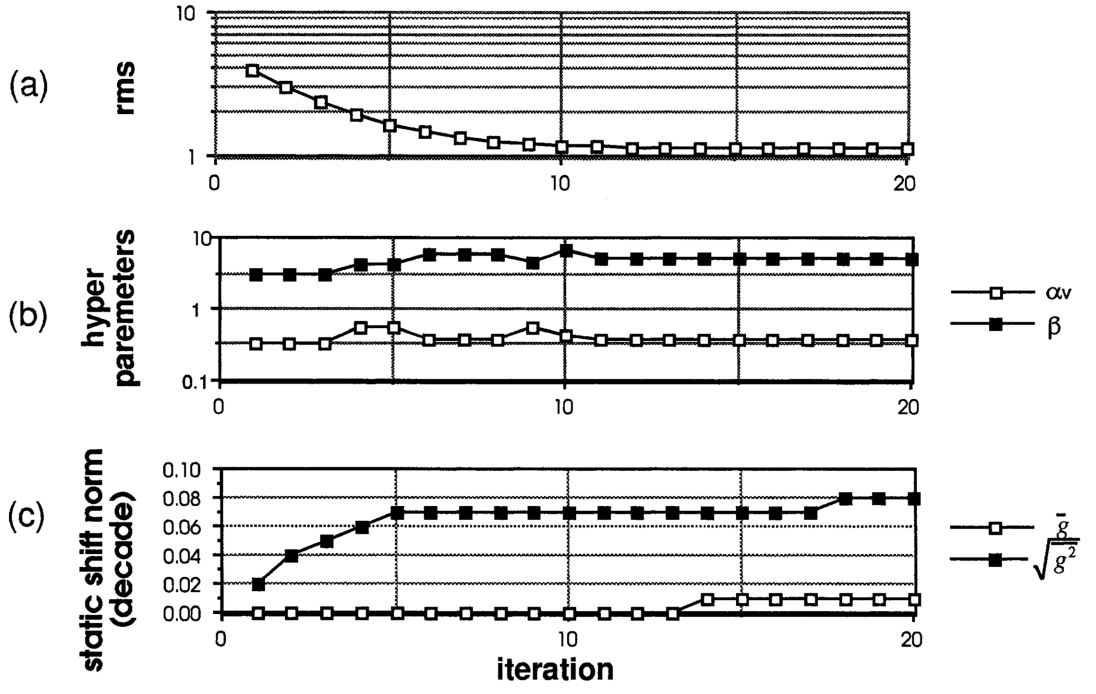

Fig. 2. (a) rms, (b) hyper parameters α_v and β, (c) static shift norm as functions of iterations.

where,

$$\tilde{d} = d - F(m_{old}) + Am_{old}. \tag{5}$$

S_0 instead of S was minimized with constraints on the following two types of norms.

The first type is model roughness, comprised of two parts: vertical roughness R_v and horizontal roughness R_h. Definitions for these roughnesses are:

$$R_v = |C_v m_\rho|^2 \tag{6}$$

and

$$R_h = |C_h m_\rho|^2. \tag{7}$$

Matrix C_v is composed of coefficients so that the i-th row of $C_v m_\rho$ represents the difference between the $\log_{10}$(resistivity) of i-th regularization block from the average of the $\log_{10}$(resistivity) of the surrounding vertically adjacent blocks. Likewise, the matrix C_h is composed of coefficients so that the i-th row of $C_h m_\rho$ represents the difference between the $\log_{10}$(resistivity) of the i-th regularization block from the average of the $\log_{10}$(resistivity) of the surrounding horizontally adjacent blocks.

The second type is the static shift $L2$ norm, G, defined as

$$G = \sum |g_{site}|^2. \tag{8}$$

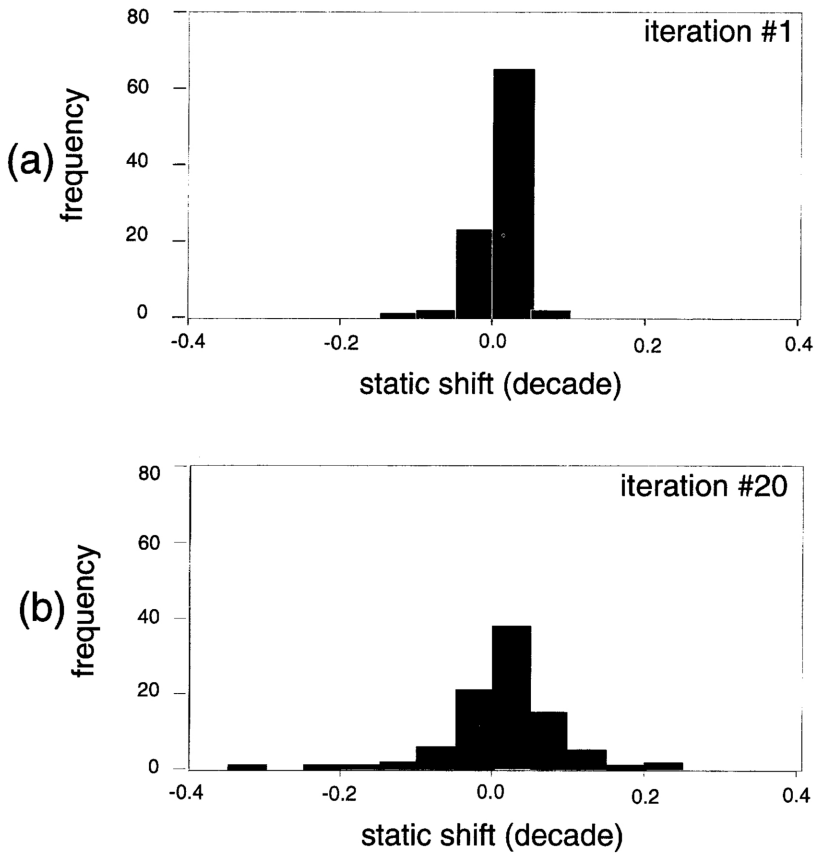

Fig. 3. Histograms of the static shifts for the first(a) and 20th(b) iterations.

Here the data misfit $S_0(m)$ was minimized with the constraints that the three norms, (1) vertical model roughness R_v, (2) horizontal model roughness R_h, and (3) the static shift norm G be simultaneously minimized. Thus the following U was minimized by using the three hyper parameters: α_v, α_h, and β.

$$U = S_0 + \alpha_v^2 R_v + \alpha_h^2 R_h + \beta^2 G. \tag{9}$$

Because of the linearization in Eq. (4), U is quadratic with respect to the model parameter m. Given proper α_h, α_h, and β, the model parameter m can be sought from the Eq. (9). In order to determine the best combination of hyper parameters, Bayesian likelihood was maximized by maximizing the Akaike's Bayesian Information Criterion (ABIC) (Akaike, 1980; Uchida, 1993a, b; Ogawa and Uchida, 1996; Ogawa, 1997). To simplify the procedure, the ratio of α_h to α_v was fixed as 3. Due to the non-linerity of the response function, the whole process was solved iteratively.

3. Application to Okemap Dataset

Since this is a large data set, only eight frequencies were used for inversion: $0.879 \cdot 10^{-2}$ Hz, $0.352 \cdot 10^{-1}$ Hz, 0.141 Hz, 0.562 Hz, 2.25 Hz, 9.00 Hz, and 36.0 Hz. The error floor for the apparent resistivity was set at 10% and an equivalent value was also set for the phase. The initial model was a half space uniform earth of 10 Ω·m, with static shifts assumed to be absent. The half space was subdivided into 37 vertical and 80 horizontal finite elements and grouped into 373 regularization blocks. The divisions of the regularization blocks are shown as black lines in Fig. 1.

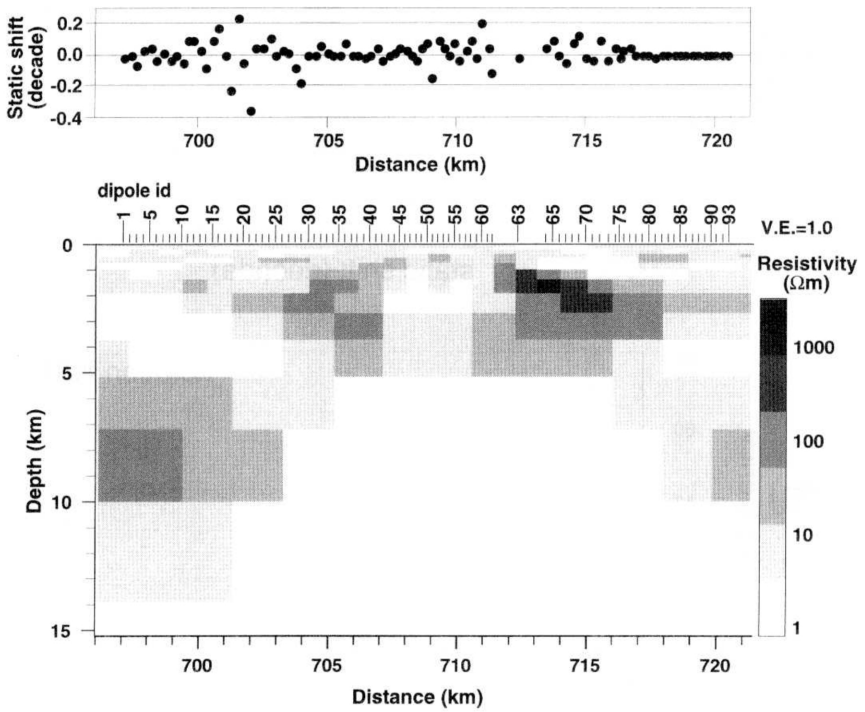

Fig. 4. The final model. The upper panel shows the static shift distribution, and the lower panel shows the resistivity model.

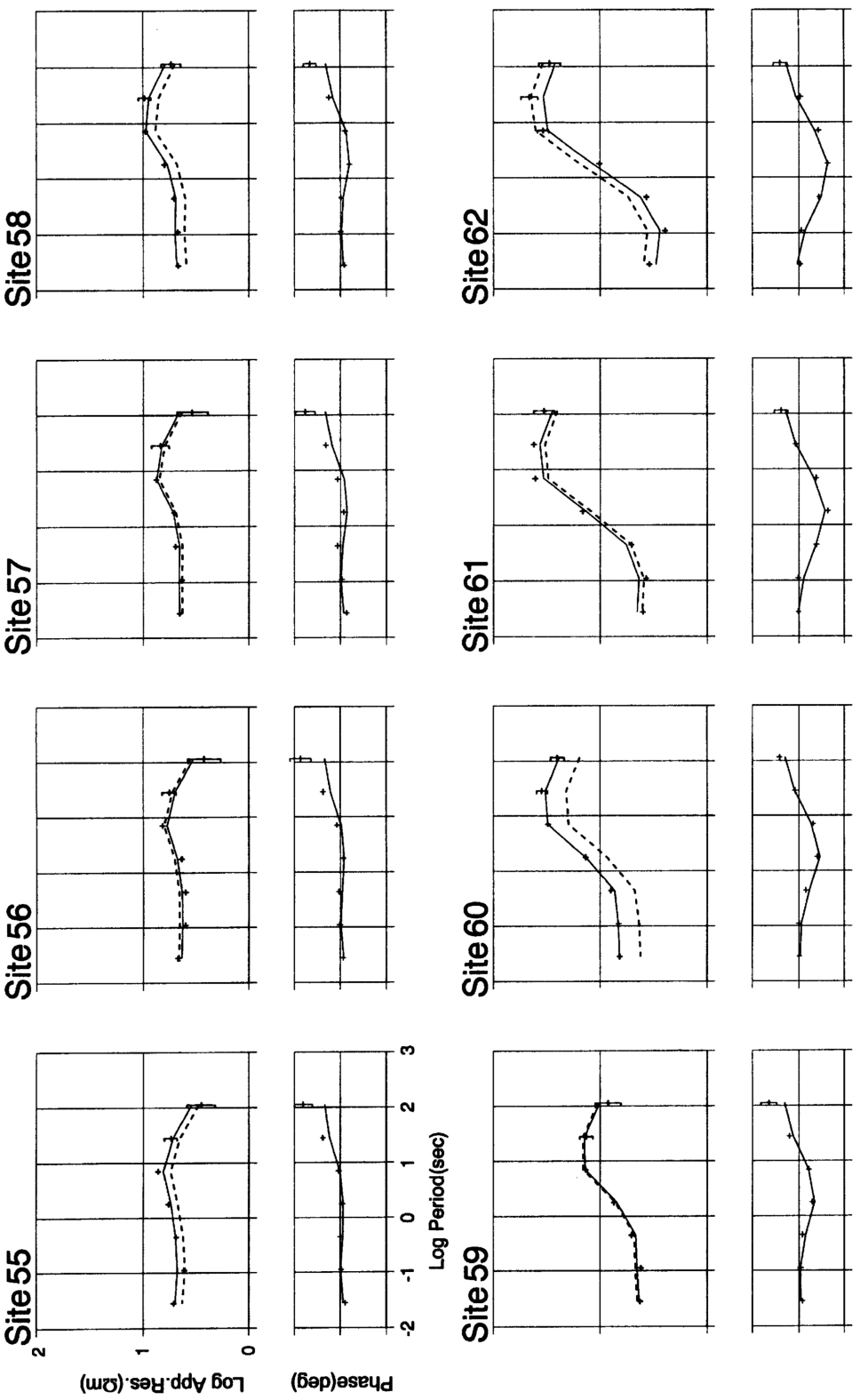

Fig. 5. Examples of observed and modeled responses between sites 55 and 62. Observed apparent resistivity and phase responses are shown by plus symbols with error bars. Modeled responses from the 20th iteration are shown by lines. Solid and broken lines in the apparent resistivity plots denote "static shift included" and "static shift removed" responses, respectively.

It should be noted that almost all surface regularization blocks have four observation sites inside them. In the TM mode, surface electric current flows horizontally across the vertical resistivity boundary and builds up electric charges at the boundary. Thus, one way for modeling static shifts is to introduce as many horizontal regularization blocks as the number of sites (see, e.g., Uchida, 1997). However, such fine regularization requires a large amount of memory for forward and inverse calculations. To alleviate the memory demand, coarse horizontal regularization division was used, and static shifts introduced.

The RMS was measured by $\sqrt{S/N}$, where N is the number of data. At the 20th iteration, RMS reached a stable value of 1.14 (Fig. 2(a)), and the hyper parameters also reached stable values of $\alpha_v = 2.58$, $\alpha_h = 7.74$, and $\beta = 5.25$ (Fig. 2(b)). It should be noted once more that the ratio of α_v to α_h was held constant (at 3). Figure 2(c) shows how the average static shift $\bar{g}$ and square root of average $L2$ norm behave with respect to iterations. The static shift $L2$ norm increases and converges to a value 0.08, while the average of static shift converges to 0.01.

Histograms of the static shifts at the first and 20th (final) iteration are plotted in Figs. 3(a) and (b) respectively. The histograms show a broader distribution of static shifts in the final model, corresponding to the increase in the $L2$ norm. Figure 4 shows the final model (20th iteration) obtained. There is an anticline structure in the center of the model. Figure 5 demonstrates typical fittings at sites 55 to 62, where static shift is relatively large and the data quality is fair. Site 60 has a positive static shift whereas site 62 has a negative one.

4. Conclusion

In this study, a two-dimensional inversion was conducted with two types of constraints similar to Ogawa and Uchida (1996). One type is model roughness norm, and the other is static shift $L2$ norm. Tradeoff parameters between misfit and constraints were chosen to maximize the Bayesian likelihood, i.e., to minimize the Akaike's Bayesian Information Criterion (ABIC). The introduction of static shift alleviated memory demand to express surface inhomogeneity. This algorithm worked well to find reasonable misfit, as well as proper model roughness and static shifts.

Alan Jones and Adam Schultz organized the second international Magnetotelluric data interpretation workshop (MT-DIW2) at University of Cambridge, UK on August, 1994. The Oklahoma EMAP dataset was made available by Exxon (USA) for the MT data interpretation workshop. This paper was prepared when the author was visiting Geological Survey of Canada, with support from the Japan International Cooperation Agency. I acknowledge Alan Jones and Jim Craven for computing facilities. Jagdish Gupta reviewed preliminary version of the manuscript. I also acknowledge the anonymous referee.

REFERENCES

Akaike, T., Likelihood and Byes procedure, in *Bayesian Statistics*, edited by J. M. Bernardo, M. H. deGroot, D. V. Lindley, and S. F. Smith, pp. 143–166, University press, Valencia, 1980.

deGroot-Hedlin, C., Removal of static shift in two dimensions by regularized inversion, *Geophys.*, **56**, 2102–2106, 1991.

Jones, A. G. and A. Schultz, Introduction to MT-DIW2 Special Issue, *J. Geomag. Geoelectr.*, **49**, this issue, 727–737, 1997.

Ogawa, Y. and T. Uchida, A two-dimensional magnetotelluric inversion assuming Gaussian static shift, *Geophys. J. Int.*, **126**, 69–76, 1996.

Ogawa, Y., Two-dimensional inversion of Papua New Guinea magnetotelluric dataset assuming static shift as Gaussian distribution, *J. Geomag. Geoelectr.*, **49**, this issue, 857–867, 1997.

Uchida, T., Smooth 2-D inversion for magnetotelluric data based on statistical criterion ABIC, *J. Geomag. Geoelectr.*, **45**, 841–858, 1993a.

Uchida, T., Inversion of COPROD2 magnetotelluric data by use of ABIC minimization method, *J. Geomag. Geoelectr.*, **45**, 1063–1071, 1993b.

Uchida, T., Two-dimensional inversion of Oklahoma EMAP data with smoothness regularization, *J. Geomag. Geoelectr.*, **49**, this issue, 791–800, 1997.